Photosynthesis Research **45:** 51–60, 1995.

Regular paper

Functional analysis of the iron-stress induced CP 43′ polypeptide of PS II in the cyanobacterium *Synechococcus* sp. PCC 7942

Stefan Falk[1], Guy Samson[2], Doug Bruce[2], Norman P.A. Huner[1,*] & David E. Laudenbach[1]
[1]*Department of Plant Sciences, University of Western Ontario, London, Ontario N6A 5B7, Canada;* [2]*Department of Biological Sciences, Brock University, St. Catharines, Ontario L2S 3A1, Canada;* **Author for correspondence and reprint requests*

Received 24 February 1995; accepted in revised form 23 June 1995

Key words: absorption cross-section, cyanobacterium, 77 K fluorescence, fluorescence decay, iron-stress, photosynthesis

Abstract

Under conditions of iron-stress, the Photosystem II associated chlorophyll *a* protein complex designated CP 43′, which is encoded by the *isiA* gene, becomes the major pigment-protein complex in *Synechococcus* sp. PCC 7942. The *isiB* gene, which is located immediately downstream of *isiA*, encodes the protein flavodoxin, which can functionally replace ferredoxin under conditions of iron stress. We have constructed two cyanobacterial insertion mutants which are lacking (i) the CP 43′ apoprotein (designated *isiA*$^-$) and (ii) flavodoxin (designated *isiB*$^-$). The function of CP 43′ was studied by comparing the cell characteristics, PS II functional absorption cross-sections and Chl *a* fluorescence parameters from the wild-type, *isiA*$^-$ and *isiB*$^-$ strains grown under iron-stressed conditions. In all strains grown under iron deprivation, the cell number doubling time was maintained despite marked changes in pigment composition and other cell characteristics. This indicates that iron-starved cells remained viable and that their altered phenotype suggests an adequate acclimation to low iron even in absence of CP 43′ and/or flavodoxin. Under both iron conditions, no differences were detected between the three strains in the functional absorption crosssection of PS II determined from single turnover flash saturation curves of Chl *a* fluorescence. This demonstrates that CP 43′ is not part of the functional light-harvesting antenna for PS II. In the wild-type and the *isiB*$^-$ strain grown under iron-deficient conditions, CP 43′ was present in the thylakoid membrane as an uncoupled Chl-protein complex. This was indicated by (1) an increase of the yield of prompt Chl *a* fluorescence (F_o) and (2) the persistence after PS II trap closure of a fast fluorescence decay component showing a maximum at 685 nm.

Abbreviations: Chl – chlorophyll; CP 43, CP 47 and CP 43′ – Chl *a* binding protein complexes of indicated molecular mass; DCMU – 3-(3,4-dichlorophenyl)-1,1-dimethylurea; F_m and F_m' – fluorescence when all PS II reaction centers are dosed in dark- and light-acclimated cells, respectively; F_o – fluorescence when all PS II reaction centers are open in dark acclimated cells; F_v – variable fluorescence after dark acclimation ($F_m - F_o$)

Introduction

While iron-stress induces a number of physiological and morphological changes in cyanobacteria, the most significant modifications are to the photosynthetic apparatus (Öquist 1971, 1974; Guikema and Sherman 1983). In cells stressed for iron, the flavin-containing flavodoxin replaces the iron-sulfur protein ferredoxin as the terminal electron acceptor of the photosynthetic electron transport chain (Hutber et al. 1977). Additionally, large variations occur in the amount of the pigment-protein complexes found in the thylakoid membranes (Guikema and Sherman 1983). The amount of all the high molecular weight Chl-protein complexes associated with PS I and PS II, as well as the number of phycobilisomes, are significantly low-

er in cells grown under iron-deficient conditions. In contrast, the small 36 kDa Chl-protein complex associated with PS II, designated CPVI-4 by Pakrasi et al. (1985b), increases dramatically in the thylakoid membranes of cells grown under iron-stress. In these cells, CPVI-4 represents the major Chl-protein complex and accounts for up to 50% of the cellular Chl content (Burnap et al. 1993). The abundance of the CPVI-4 polypeptide in the thylakoid membrane of iron-starved cells is reflected by a characteristic blue-shift of the Chl *a* absorbance peak of about 5 nm and by a dominant 77 K fluorescence emission peak centered around 685 nm (Guikema and Sherman 1983; Burnap et al. 1993; Pakrasi et al. 1985a,b; Riethman et al. 1988).

An iron stress-induced operon containing the *isiA* and *isiB* genes has been characterized in the cyanobacterium *Synechococcus* sp. PCC 7942 (Laudenbach and Straus 1988; Laudenbach et al. 1988). The *isiB* gene, which is located immediately downstream of *isiA*, was shown to encode flavodoxin. Additionally, the *isiA* gene exhibited similarity to the *psbC* gene that encodes the PS II Chl-binding protein CP 43 and indirect evidence from these studies suggested *isiA* encoded the 36 kDa apoprotein of the CPVI-4 complex. More recently, Burnap et al. (1993) have constructed a mutant strain of *Synechococcus* sp. PCC 7942 where the *isiAB* operon has been inactivated by insertional mutagenesis. Using a non-denaturing, low ionic strength acrylamide gel system, these investigators demonstrated that this mutant no longer expressed the CPVI-4 complex (which was renamed CP 43′). The blue shift of the Chl *a* absorbance peak and the dominant 685 nm fluorescence emission peak were absent in the *isiA*$^-$-strain grown under iron stress (Burnap et al. 1993).

The function of CP 43′ still remains to be elucidated and three possibilities have been proposed in the literature. Originally, Pakrasi et al. (1985b) postulated that this complex might act as an alternate antenna complex for PS II in the replacement of the phycobilisomes lost due to iron deprivation. They also discussed the possibility that CP 43′ could be a functionally important component of the PS II reaction center. From its sequence similarity with CP 43, it has also been suggested that CP 43′ may serve as a functional replacement for CP 43 in iron-deficient cells (Burnap et al. 1993). Other observations indicate that CP 43′ might also function as a storage protein for Chl under iron-deficient conditions that can be reorganized into new complexes synthesized as cells reacquire iron reserves (Troyan et al. 1989; Riethman et al. 1988; Burnap et al. 1993).

In order to examine unequivocally the function of the CP 43′ complex, we have constructed two *Synechococcus* sp. PCC 7942 mutant strains containing interrupted copies of the *isiA* and *isiB* genes. In this report, we focused our attention on the possibility that CP 43′ acts as an alternate PS II light-harvesting complex. We measured the PS II functional absorption cross-section and analyzed the ps fluorescence decay kinetics in the wild-type and the two mutant strains grown under optimal or iron-deficient concentrations. Our results indicate that CP 43′ is not part of the PS II functional light-harvesting system.

Materials and methods

Culture conditions

Cells of *Synechococcus* sp. PCC 7942 SPC (small plasmid cured) were pre-grown axenically, at 10^{-17} M (optimal) and 10^{-21} M available Fe in modified BG-11 medium (Allen 1968) supplemented with 10 mM TES (N-tris[hydroxymethyl]methyl-2-aminoethanesulfonic acid), pH 8.0 as described in Laudenbach et al. (1988). The phosphate stock-solution, which has a relatively high level of iron-contamination, was treated in a separate Chelex-100 column prior to use. Concentrations of iron added to the medium were determined by the method of Westall et al. (1976) and represent the available level of iron initially present in the growth media.

Experimental cells were taken in late log-phase of growth and transferred to 50 ml of fresh growth medium in test-tubes of 25 mm diameter at a cell density of approximately 5×10^7 cells ml^{-1}. These tubes were immersed in a glass-sided aquarium thermostated at 29 °C. 30 μmol m^{-2} s^{-1} of light (as measured in the culture tube), which is saturating for growth, was provided by a bank of incandescent light-bulbs. Five percent CO_2 (g) in air was fed aseptically to the tubes to achieve maximum growth rates and provide stirring inside the test-tube. Cells at mid-log phase of growth were used in all experiments.

Deletion inactivation of the isiA *and* isiB *genes*

A 2.9 kb *Bgl*II restriction fragment, containing the *isiAB* operon (Laudenbach et al. 1988), was cloned into the *Bam*HI site of pUC9 (designated pFVBS) and used for subsequent constructions. To inactivate *isiA*, the pHP45Ω Sp resistance gene (Prenti and Krisch

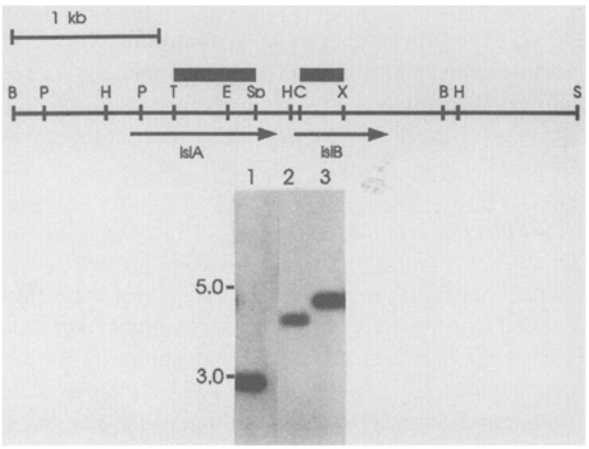

Fig. 1. Insertional mutagenesis of the *isiAB* operon in *Synechococcus* sp. PCC 7942. The restriction map of the *isiAB* operon shown above has been described previously (Laudenbach et al. 1988). The restriction endonuclease sites are abbreviated as follows; B *Bgl*II; P, *Pst*I; H, *Hind*III; T, *Stu*I; E, *Eco*RI; Sp, *Sph*I; C, *Cla*I; X, *Xba*I, S, *Sac*I. The position of the open reading frames, their gene designations and the direction in which they are transcribed (indicated with arrows) are given below the map. The sites of gene deletion are indicated above the restriction map with a filled rectangle. The spectinomycin resistance gene was inserted in the same direction as the interrupted gene is transcribed. A DNA gel blot hybridization with DNA from the *isiA* and the *isiB* mutant strains is shown below the restriction map. Genomic DNA from the wild-type strain (lane 1), the *isiA*$^-$-mutant (lane 2) and the *isiB*$^-$-mutant (lane 3) was digested with *Bgl*II, electraphoresed on a 0.7% agarose gel and transferred onto a nitrocellulose filter. The immobilized DNA was hybridized with a 2.9 kb *Bgl*II fragment, labeled with [α-P^{32}] dCTP, containing the entire coding region of the *isiAB* operon. Size markers, to the left of the autoradiogram, are shown in kilobase pairs.

1984) was ligated into the *Stu*I/*Sph*I site (made blunt with T4 DNA polymerase) of pFVB5 (Fig. 1) and electroporated into *E. coli* DH10B cells. To inactivate *isiB*, the Sp resistance gene was ligated into the *Cla*I/*Xba*I sites of pFVB5, made blunt with the Klenow fragment of *E. coli* DNA polymerase I, and electroporated into *E. coli* DH10B cells. Plasmid DNA from the *isiA* and *isiB* inactivation constructs were used to transform *Synechococcus* sp. PCC 7942 to Sp^R (20 μg/ml) by the method of Laudenbach et al. (1988).

Isolation and analysis of chromosomal DNA

Total genomic DNA was extracted from *Synechococcus* sp. PCC 7942 as described previously (Laudenbach et al. 1988). Radio-labeled probes were obtained using a Quick Prime Kit (Pharmacia) and [α-^{32}P)dCTP according to the manufacturers instructions. DNA gel blot analysis was carried out as described in Sambrook et al. (1989).

Growth rates, Chl a and phycobilisome determinations

Growth rates under autotrophic conditions were determined microscopically by direct counting of cells in a Bürker-chamber. Chl *a* was determined using the equations of Porra et al. (1989) and PBS content was determined as in Zhao and Brand (1989). All absorbance values and absorption spectra were recorded on a Shimadzu MPS-250 spectrophotometer at a half bandwidth of 2 nm. Sample turbidity was determined at 750 nm.

Photosynthetic oxygen evolution

Photosynthetic oxygen evolution was determined polarographically using a Clark-type electrode (Hansatech Ltd., King's Lynn, UK). The Chl concentration was less, than 7 μg Chl ml^{-1} and all samples were provided with 4 mM $NaHCO_3$. Photosynthetic rates were determined at 10 irradiances ranging from 0 to 2000 μmol m^{-2} s^{-1}. The data were fitted to the equation in Leverenz et al. (1990) from which the resulting parameters for dark respiration (R_D) and maximum rate of photosynthesis (P_{max}) were calculated.

Chlorophyll fluorescence measurements

Room temperature fluorescence signals from samples of intact cells, were generated by a pulse-amplitude modulated fluorometer (PAM Chlorophyll fluorometer 101, Heinz Walz GmbH, Effeltrich, Germany) using the PAM 103 accessory and two Schott-lamps: one to provide saturating flashes and a second to provide continuous actinic illumination. Samples were transferred to a temperature controlled, liquid phase cuvette (KS 101, Heinz Walz) before the onset of illumination.

The 77 K fluorescence spectra were measured on intact cells that were dark-adapted prior to freezing in NMR-tubes of 4 mm diameter. 77 K-spectra were recorded using a luminescence spectrophotometer (LS-1, Photon Technology International Inc., South Brunswick, NJ, USA) at an excitation wavelength of 425 nm for Chl *a*-excitation (half-bandwidth 25 nm). Fluorescence emission was detected at a half-bandwidth of 4 nm in samples having a final Chl *a* content of less than 10 μg ml^{-1}, as described in Krupa

et al. (1992). The fluorescence emission spectra were normalized for the emission peak at 712 to 716 nm.

Time-resolved fluorescence decay

Fluorescence decay kinetics were measured with a picosecond time-resolved photon timing apparatus described in detail by Bruce and Miners (1993). Excitation pulses were supplied by a Hamamatsu PLP-01 pulsed laser diode at an excitation wavelength of 665 nm, with a pulse width of approximately 60 ps. The photon flux incident on the sample was 3.5×10^8 photons cm^{-2} $pulse^{-1}$. Fluorescence was detected at a 90° angle to the incoming excitation. The sample was held at room temperature in a flow cell of 2 × 5 × 20 mm with a total volume of 200 µl, with the short-side facing the excitation beam. On the fluorescence detection side, a mask covered all but a 1 mm opening at the center of the excitation beam. Dark-adapted cells were circulated at a flow rate of 30 ml min^{-1} through the cuvette by a peristaltic pump during the collection of data with PS II in an open state (F_o-conditions), while a final concentration of 20 µM DCMU was added to cells in a non-circulating cuvette exposed to bright light before the collection of data with PS II in a closed configuration (F_m-conditions). Furthermore, to avoid reopening of PS II during measurements at the F_m-conditions, light (15 µmol m^{-2} s^{-1}) was applied through a Schott BG-39 glass filter during the measurement. The Chl *a* concentration was 2.1 to 3.8 µg ml^{-1} for cells grown at 10^{-17} M Fe and 0.5 to 1.1 µg ml^{-1} for cells grown at 10^{-21} M Fe. Data collection was controlled by a multi channel pulse height analyzer (The Nucleus PCAII board). The instrument response functions were obtained by setting the detection monochromator to the excitation wavelength (665 nm) and collecting data from a suspension of latex beads (1.09 µm diameter, Marivac Ltd., Halifax, N.S., Canada) in the growth medium. Fluorescence decay data contained 512 channels and were collected to 10^4 counts in the peak channel. Time per channel was 12.34 ps. For each experiment, five individual fluorescence decay curves were collected at 5 nm intervals from 680 nm to 700 nm. The fluorescence decay data were fitted by modeling with a convolution of the instrument response function to a sum of exponential decay components. All decay curves were modeled simultaneously with a global fitting routine used to determine decay-associated spectra. This procedure optimizes a global fit of data at all emission wavelengths and assumes the component lifetimes to have an invariant wavelength (Wendler and Holzwarth 1987). The fitting program used an optimized Levenberg/Marquat algorithm and was developed by Warren Zipfel (ICS, Ithaca, NY). Unless otherwise noted the uncertainty in all reported lifetimes and amplitudes was 15%.

PS II absorption cross-section

Functional PS II cross-sections (σPS II) for the different cell cultures were determined from light saturation curves of Chl *a* fluorescence using the pump-probe fluorimeter described in Falk et al. (1994). Samples were transferred directly from the cultures to a 1 × 1 cm glass cuvette held in a water jacketed cuvette holder at 29 °C. The samples contained less than 2.1 µg ml^{-1} and 0.45 µg ml^{-1} Chl *a* for the cells grown at 10^{-17} M Fe and 10^{-21} M Fe, respectively. Chl *a* fluorescence yield, induced by a weak Xenon flash fired 50 µs after an actinic laser flash (250 ns duration), was averaged after 24 flashes provided at a frequency of 0.25 Hz. The actinic laser pulse was set at 673 nm. During measurements, cells were illuminated with a far red light (720 nm, half bandwidth of 13 nm) at an intensity of 15 W m^{-2} in order to stabilize cells in state 1 and to maximize variable Chl *a* fluorescence. Values of σPS II were estimated from the fit of the data using the cumulative single hit Poisson distribution equation (Ley and Mauzerall 1982).

Results and discussion

Insertional Inactivation of isiA *and* isiB

The *isiA* gene is predicted to encode a protein of 36 kDa with significant similarity to the amino acid sequence of the Photosystem II Chl binding protein CP 43, which is encoded by the *psbC* gene. Recently, the *isiA* gene has been shown to encode the iron-regulated apoprotein of the Photosystem II Chl-protein complex, CPVI-4 (renamed CP 43′ by Burnap et al. 1993). The *isiB* gene, which is located immediately downstream of *isiA* (Laudenbach et al. 1988), encodes the protein flavodoxin, which can functionally replace ferredoxin under conditions of iron stress (Hutber et al. 1977). In order to determine the function of the CP 43′ Chl complex, we used cartridge mutagenesis to construct in vitro deletion derivatives of the clone pFVBS in which either *isiA* or *isiB* were interrupted by a gene that confers resistance to spectinomycin (Fig. 1). Since the inser-

tion of the Ω element of pHP45Ω in *isiA* also effectively prevents the accumulation of detectable transcripts corresponding to the *isiB* gene (data not shown, Burnap et al. 1993), the *isiB*-strain was used as a control so that mutant phenotypes could be attributed to either the lack of CP 43′ or flavodoxin. These constructs were used to transform wild-type cells of *Synechococcus* sp. PCC 7942 to spectinomycin resistance. Since the constructs were originally cloned in pUC9, an *E. coli* plasmid that cannot replicate in *Synechococcus* sp. PCC 7942 SPC, spectinomycin resistance must result from the integration of the plasmid DNA into the cyanobacterial genome. The resulting Sp^R transformants were screened for sensitivity to ampicillin (1 μg/ml), a phenotype indicative of a double, homologous recombination that would replace the wild-type *isiA* and *isiB* genes with the interrupted sequences (Golden et al. 1986). Ampicillin-resistant transformants, probably the result of a single recombinational event, were not analyzed further.

After the purification of homozygous mutants (Williams 1988), genomic DNA was isolated, digested with the appropriate restriction enzymes and analyzed by DNA gel blot hybridizations. The restriction fragments of genomic DNA from the two mutant strains were the sizes expected from a double, homologous recombination event. As shown in Fig. 1, the *isiA*$^-$ and *isiB*$^-$-strains hybridized to 4.4 kb and 4.7 kb *Bgl*II restriction fragments, respectively. Wild-type copies of the DNA (Fig. 1, lane 1) were not detected in either mutant strain, indicating that these mutant strains had segregated to pure, stable cultures.

Cell characteristics

Wild-type, *isiA*$^-$, and *isiB*$^-$-strains of *Synechococcus* sp. PCC 7942 exhibited similar maximum growth rates (μ_{max}), Chl *a* and PBS contents per cell and the same position of the Chl *a* absorbance peak when grown under iron-sufficient (10^{-17} M Fe) conditions (Table 1). Consistent with previous reports (Hardie et al. 1983; Sandmann 1985), growth at iron-stressed (10^{-21} M Fe) conditions resulted in a reduction in cell size (data not shown) as well as Chl *a* and PBS content per cell. In the wild-type and *isiB*$^-$-strains grown at 10^{-21} M Fe, the ratio of Chl *a*/PBS increased 4-fold relative to cells grown at 10^{-17} M Fe and the Chl *a* absorbance peak was blue-shifted by 4–6 nm (Table 1). In *isiA*$^-$ cells grown at 10^{-21} M Fe, the presence of PBS was not detected. In those cells, the Chl *a* absorbance peak remained at 678 nm as previously reported (Burnap et al. 1993), confirming that the blue shift of the Chl *a* peak at low iron concentration reflects the presence of CP 43′ as the major Chl-protein complex in the cells. We also noted that the absence of the CP 43′ polypeptide in iron-stressed *isiA*$^-$ cells of *Synechococcus* sp. PCC 7942 reduced its photosynthetic capacity by about 40% which was similar to that observed for the wild-type and *isiB*$^-$-strains (Table 1). In addition, there was a strong increase in dark respiration. However, these results are biased by the fact that growth under iron-stressed conditions resulted in a 70 to 90% reduction in the Chl *a* content (Table 1). Although the cell doubling times of the three strains were only slightly affected by iron deprivation, their reduced cell sizes imply that the overall rate of biomass production under these conditions was less than at 10^{-17} M Fe (Table 1). Thus, our results indicate that cells grown at 10^{-21} M Fe remained photosynthetically competent and that their altered phenotype suggests an adequate acclimation to iron-stress even in absence of CP 43′ and/or flavodoxin. The normal growth of the two mutants at 10^{-21} M Fe indicates the residual presence of ferredoxin is not a limiting factor for growth under the conditions tested.

When iron was added to cells maintained at stationary growth in media supplied with 10^{-21} M Fe, it was observed that the *isiA*$^-$-strain had a longer lag-time than wild-type cells before exponential growth was obtained (data not shown) This is consistent with the data of Burnap et al. (1993). Repletion of iron to cells of a single *isiB*$^-$-mutation, lacking only the iron-stress induced flavodoxin, resulted in no difference in growth rates when compared to wild-type cells (data not shown) indicating that it is indeed the exclusion of CP 43′ in the *isiA*$^-$-strain that alters the growth response.

Figure 2 shows 77 K fluorescence emission spectra for dark adapted cells of *Synechococcus* sp. PCC 7942 excited at the absorption peak of Chl *a* (425 nm). Emission peaks or shoulders are observed at 655 nm (phycocyanin), 682 nm (Chl *a* antenna and PS II reaction centre), 695 nm (CP 47 of PS II reaction centre) and approximately 715 nm (low energy antenna Chl *a* associated with PS I). Spectra for wild-type and mutant cells grown at 10^{-17} M Fe (Fig. 2a) are similar and are dominated by the PS I emission at 715 nm (a 715/682 nm peak ratio of 3.3 to 4.1) which qualitatively reflects the high PS I/PS II ratio usually found in these cells. Growth at 10^{-21} M Fe (Fig. 2b) causes a dramatic change in the emission spectra of wild-type and *isiB*$^-$ cells. The 715/682 nm fluorescence emis-

Table 1. Cells characteristics for the wild-type, *isiB*$^-$ and *isiA*$^-$-mutant cells of *Synechococcus* sp. PCC 7942 grown at 10^{-17} and 10^{-21} M available Fe. The maximum growth rate (μ_{max}) was determined as the doubling time in h. Chl *a* and PBS content was calculated as fg and arbitrary units cell^{-1} ± SE, respectively. Maximum rate of photosynthesis (P_{max}) and dark respiration (R_D) are presented as μmol O_2 (mg Chl *a*)$^{-1}$ h^{-1}. The parameters were obtained by fitting the data to the model in Leverenz et al. (1990). nd = not detected

Cell type	Available Fe (M)	μ_{max} (h)	Chl *a* cell^{-1} (fg)	PBS cell^{-1} (a.u.)	Chl *a*/PBS	Chl *a* A peak (nm)	P_{max}	R_D
Wild-type	10^{-17}	8.6	19.85 ± 1.60	82.30 ± 0.71	0.24	678	276	−40
isiB$^-$		7.2	12.80 ± 0.73	60.37 ± 0.55	0.21	678	226	−38
isiA$^-$		8.6	15.20 ± 1.28	68.30 ± 0.71	0.22	678	281	−65
Wild-type	10^{-21}	8.0	4.26 ± 0.98	4.35 ± 2.01	0.98	672	149	−62
isiB$^-$		9.0	3.72 ± 0.26	4.18 ± 0.89	0.89	674	160	−65
isiA$^-$		9.5	1.85 ± 0.20	nd	–	678	163	−156

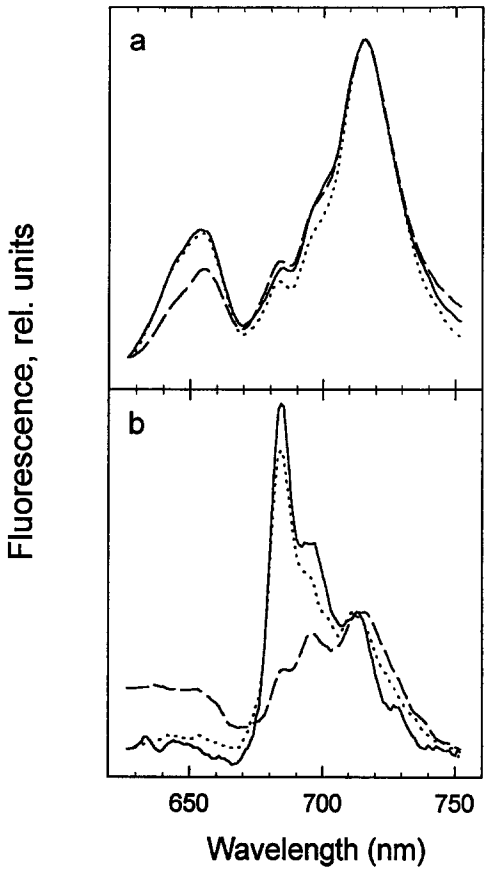

Fig. 2. Representative 77 K fluorescence emission spectra for intact wild-type (solid line), *isiA*$^-$-(dashed line) and *isiB*$^-$-mutant (dotted line) cells of *Synechococcus* sp. PCC 7942 grown at (a) 10^{-17} and (b) 10^{-21} M available Fe. Fluorescence was excited at 425 nm at a half bandwidth of 25 nm. Spectra were normalized to their maximum fluorescence emission peak at 712 to 716 nm.

Table 2. Functional absorption cross-sections of PS II (σPS II) measured at 673 nm and Chl *a* fluorescence ratios determined with a pump-probe fluorimeter for the wild-type, *isiB*$^-$ and *isiA*$^-$-mutant cells of *Synechococcus* sp. PCC 7942 grown at 10^{-17} and 10^{21} M available Fe

Cell type	Available Fe (M)	σPS II (Å^2 ± SE)	F_v/F_0	F_0/[Chl *a*] arb. units
Wild-type	10^{-17}	37.4 ± 6.5	0.55 ± 0.17	4.0 ± 0.2
isiB$^-$		37.2 ± 3.5	0.73 ± 0.07	3.8 ± 0.8
isiA$^-$		38.7 ± 7.1	0.53 ± 0.03	4.2 ± 0.8
Wild-type	10^{-21}	31.5 ± 8.6	0.47 ± 0.09	8.0 ± 0.9
isiB$^-$		34.5 ± 3.5	0.40 ± 0.05	6.3 ± 0.4
isiA$^-$		35.9 ± 7.3	0.67 ± 0.01	4.4 ± 0.6

sion peak ratio decreased to 0.40 and 0.46, suggesting a strong reduction in PS I content relative to PS II. As shown previously (Burnap et al. 1993) growth at low iron does not cause this large increase in the fluorescence emission ratio in the *isiA*$^-$ cells (lacking CP 43′). The *isiA*$^-$-strain exhibits a minor decrease in the relative emission from PS I as compared to PS II (715/682 nm fluorescence ratio of 1.7) when compared to cells grown at 10^{-17} M Fe. The dominance of the 682 nm peak in the emission spectra of the wild type and the *isiB*$^-$-strain grown at 10^{-21} M Fe, as well as the blue shift of the Chl *a* absorbance peak (Table 1), are therefore correlated with the presence of CP 43′ and not flavodoxin in these cells.

Functional PS II absorption cross sections

Light saturation curves of variable Chl *a* fluorescence induced from single turnover flash were measured for the three strains grown at both optimal and iron-deficient concentrations. Chl *a* fluorescence yield parameters and the values of σPS II determined from the fit of the data to Eq. (1) are presented in Table 2. Remarkably, no differences in the σPS II values were found between the different strains or between the cells grown at high or low iron concentrations. These results indicate that (1) the CP 43′ polypeptide is not a part of the functional PS II antenna and that (2) the PS II photosynthetic unit is not significantly affected by the changes of the Chl-protein organization induced by iron-stress.

It is noteworthy that when compared to cell cultures grown at 10^{-17} M Fe, the wild-type and *isiB*$^-$-strains grown at 10^{-21} M Fe had an increased level of prompt fluorescence F_o emitted for a same concentration of Chl *a* whereas the *isiA*$^-$-strain maintained a similar F_o/[Chl *a*] ratio (Table 2). This contributed to a depressed F_v/F_o ratio in the iron-starved wild-type and the *isiB*$^-$ cells, as previously reported (Guikema and Sherman 1983). It was suggested that this increased level of F_o might reflect the presence of CP 43′ polypeptides uncoupled or poorly coupled to the Photosystem core pigment beds (Riethman and Sherman 1988).

Picosecond fluorescence decay kinetics

To further investigate the energetic coupling of CP 43′ to the PS II reaction centre, we analyzed the time resolved fluorescence decay kinetics from the different cell cultures grown at 10^{17} and 10^{-21} M Fe. With the exception of wild-type and *isiB*$^-$ cells grown at 10^{-21} M Fe measured under F_m-conditions (Figs. 3d and f), both individual as well as global fits of the data required five exponential fluorescence decay components under F_o- and four components under F_m-conditions as judged from individual and global χ^2-determination and residuals analyses. All strains grown under iron-sufficient conditions exhibited, as expected, a high degree of similarity in both amplitude and lifetime of the fluorescence decay components (represented by the wild-type data, Figs. 3a and b).

The longest-lived decay component (1.5 to 3.5 ns) was of very low amplitude in all cases, similar to previous results presented by Mullineaux and Holzwarth (1991) and Bittersman and Vermaas (1991). In all experiments, the largest contribution to the total decay

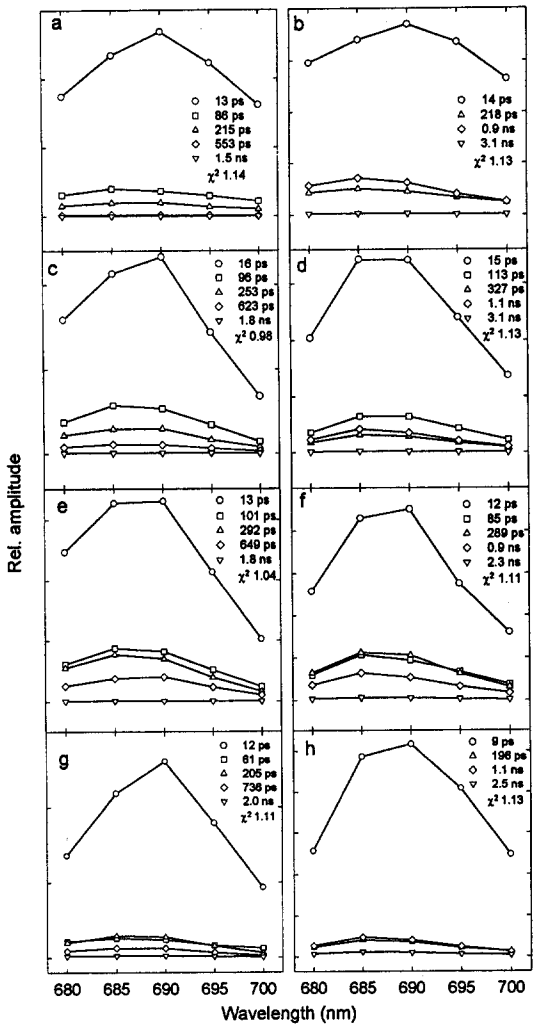

Fig. 3. Decay-associated fluorescence emission spectra for intact wild-type (panels a, b, c and d), *isiB*$^-$-mutant (panels e and f) and *isiA*$^-$-mutant (panels g and h) cells of *Synechococcus* sp. PCC 7942 grown at 10^{-17} (panels a and b) and 10^{-21} (panels c to h) M available Fe. Data were recorded with PS II-traps in dark-adapted F_o- (panels to the left) or F_m-state in the presence of DCMU (panels to the right). Excitation was at 665 nm. The deconvoluted fluorescence lifetime components and the global X2 are indicated in each panel.

was associated with the fastest decay component which had a lifetime of 10 to 15 ps (Fig. 3, circles). The relative contribution of this component was not significantly different between F_o and F_m and the peak amplitude in the decay associated spectra was 690 nm in all cases. These two characteristics are indicative of a PS I origin for this component. The lifetime of this PS I decay component is faster than previously reported (30–40 ps) in cyanobacteria (Mullineaux and Holzwarth 1991). However, these fast lifetimes are at

the limit of resolution of our system and carry a relatively large uncertainty (20 ps).

The second largest contribution to the decay in all cells at F_o was from a component with a lifetime ranging from 60 to 100 ps. This decay component was maximum at 685 nm and, in all cells grown at 10^{-17} M Fe, was completely replaced by a much slower decay component (approximately 1 ns) upon PS II trap closure at the F_m level. The complete replacement of this fast PS II decay component with a slow decay component was also observed in *isiA*$^-$ cells grown at low iron levels. These characteristics are consistent with previous studies of fluorescence decay kinetics in cyanobacteria based on the exciton-radical pair model for PS II (Mullineaux and Holzwarth 1991), where similar fast and slow decay components were assigned to energy transfer and trapping processes in open and closed PS II centres respectively. Figures 3d and 3f, clearly show wild-type and *isiB*$^-$ cells grown at low iron to have a larger contribution of this fast PS II decay component at F_o. In addition, only about 30% of this component was lost upon trap closure in these cells in contrast to the complete loss observed in all cells grown at high iron levels and the *isiA*$^-$ cells grown at low iron levels. Both the increased contribution of the fast decay component (60 to 100 ps) and its persistence upon trap closure (F_m) were therefore correlated with the presence of CP 43′ in wild-type and *isiB*$^-$ cells grown at low iron levels. The lifetime of the fast PS II component at F_o was not significantly different between wild-type and mutant cells grown at either high or low iron.

Two additional components were used in the modeling of the decay kinetics. A component with a 200 ps to 300 ps lifetime with a broad emission maximum in the region of 685–690 nm was observed in all cells under all conditions (Fig. 3). This component was largely unaffected by trap closure or growth at low iron. The other intermediate lifetime component had a low amplitude with a 550–750 ps lifetime and was observed in all cells at F_o. This component disappeared upon trap closure (F_m) in all cells at high and low iron. Intermediate lifetime components with similar and somewhat shorter lifetimes which disappear upon trap closure have been previously observed in cyanobacteria at F_o and have been attributed to charge stabilization in PS II (Mullineaux and Holzwarth 1991).

The persistence of the 60–100 ps component under F_m conditions was observed only in iron-starved cells of the wild-type and the *isiB*$^-$-strain where the CP 43′ polypeptide represents the major Chl-protein complex. This observation could indicate an incomplete PS II trap closure in those cells, however the disappearance in all experiments under F_m conditions of the component attributed to charge stabilization in PS II (550–750 ps lifetime) suggests that complete trap closure was obtained in all strains grown at 10^{-17} and 10^{-21} M Fe. As shown by our absorbance cross-section determinations, the large amounts of CP 43′ present in the wild type and the *isiB*$^-$-strain at low iron are not energetically coupled to PS II. We therefore assign the portion of the 60 to 100 ps component that was unaffected by trap closure in iron-stressed wild-type and *isiB*$^-$ cells to energetically uncoupled CP 43′. This assignment is consistent with an efficient quenching of excitation energy and conversion to heat in these uncoupled Chl-protein complexes.

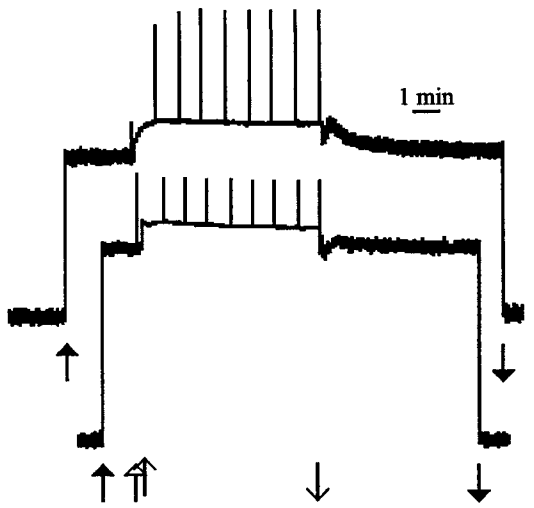

Fig. 4. Representative recordings of room temperature Chl *a* fluorescence induction for intact wildtype cells of *Synechococcus* sp. PCC 7942 grown at 10^{-17} (upper trace) and 10^{-21} M (lower trace). Arrows indicate probing beam on (↑) and off (↓), saturating flash (↑) and continuous actinic light on (↑) and off (↓). The irradiance of continuous actinic light was 59 μmol m^{-2} s^{-1}.

Room temperature modulated fluorescence

Finally, we examined the possibility that the reorganization of the thylakoid membrane and the abundance of CP 43′ in cells grown under iron-stress might affect the phenomenon of state transitions. Figure 4 shows that the fully dark-adapted room temperature F_m-level of fluorescence was strongly quenched in wild-type cells of *Synechococcus* sp. PCC 7942 grown at 10^{-17} M Fe. This is consistent with the observation that dark-adapted cyanobacterial cells are usually in

state 2 (Mullineaux and Allen 1986) which is characterized by a low PS II fluorescence yield. Upon illumination of these cells for less than 2 min at 58 μmol m^{-2} s^{-1} of white, light, the quenching was released and fluorescence increased to a higher level F_m, characteristic of cells in state 1. Subsequently, F_m increased to a higher level, $F_{m'}$, characteristic of cells in state 1. Similar observations were made with the two mutants grown at 10^{-17} M Fe (data not shown). However, all cells grown at 10^{-21} M Fe did not display any detectable state transition, indicating that the CP 43′ polypeptide plays no role in the mechanism. Furthermore, the F_m-level recorded in these dark-adapted cells was always higher than any $F_{m'}$-peak recorded under white actinic light (Fig. 4). From their relatively high ratio of F_m/F_o, it appears that the dark-adapted iron-starved cells are found in state 1.

Conclusions

The results presented in this report allow us to conclude unequivocally that the CP 43′ polypeptide present in cyanobacterial cells grown under iron-stress does not contribute to the PS II light-harvesting system. There were no differences in the PS II functional absorption cross-sections in the wild-type and the *isiA*$^-$ and *isiB*$^-$ cells grown at both optimal and iron-deficient concentrations. The presence of CP 43′ in the thylakoid membrane as an uncoupled Chl-protein complex was indicated by an increased level of prompt F_o fluorescence and also by the presence of a fast (approximately 100 ps) fluorescence decay component under F_m conditions in cells where CP 43′ was the dominant Chl-protein complex. Therefore, it is unlikely that CP 43′ can replace CP 43 as a proximal PS II antenna component as recently suggested (Burnap et al. 1993).

The increased lag time observed after iron addition to retrieve exponential growth rate in iron-deprived *isiA*- cultures (our results; Burnap et al. 1993) is in agreement with the idea that the CP 43′ polypeptide contributes in the process of cell recovery from iron deprivation. In iron-starved cells where Chl biosynthesis was inhibited with gabaculine, it was previously shown that after addition of iron, new Chl-protein complexes CP 43 and CP 47 were synthesized (Troyan et al. 1989). Changes in the 77 K Chl fluorescence emission spectrum (Riethman and Sherman 1988) as well as the absorbance spectrum (Guikema et al. 1986) characteristic of recovery from iron deprivation were also reported. From all these observations, it appears that the most easily seen function of the CP 43′ polypeptide is to provide Chl *a* molecules to other Chl-protein complexes synthesized during recovery from iron deprivation. Further work is required to substantiate this hypothesis.

Acknowledgements

This research was supported by NSERC Research Grants to NPAH, DB and DEL. SF was funded by a NSERC International Postdoctoral Fellowship. This paper is dedicated to the memory of DEL who died on June 16, 1995.

References

Allen M (1968) Simple conditions for growth of unicellular blue-green algae on plates. J Phycol 4: 1–3

Bittersman E and Vermaas W (1991) Fluorescence lifetime studies of cyanobacterial Photosystem-II mutants. Biochem Biophys Acta 1098: 105–116

Bruce D and Miners J (1993) Use of a pulsed laser diode to measure picosecond fluorescence lifetimes. Photochem Photobiol 58: 464–468

Burnap RL, Troyan T and Sherman LA (1993) The highly abundant chlorophyll-protein complex of iron-deficient *Synechococcus* sp. PCC 7942 (CP 43′) is encoded by the *isiA* gene. Plant Physiol 103: 893–902

Falk S, Bruce D and Huner NPA (1994) Photosynthetic performance and fluorescence in relation to antenna size and absorption cross-sections in rye and barley grown under normal and intermittent light conditions. Photosynth Res 42: 145–155

Golden S S, Brusslan J and Haselkorn R (1986) Expression of a family of lit psbA genes encoding a Photosystem II polypeptide in the cyanobacterium *Anacystis nidulans* R2. EMBO J 4: 2789–2798

Guikema JA and Sherman LA (1983) Organization and function of chlorophyll in membranes of cyanobacteria during iron starvation. Plant Physiol 73: 250–256

Guikema JA, Freeman L and Fleming EH (1986) Effects of gabaculine on the pigment biosynthesis in normal and nutirent deficient cells of *Anacystis nidulans*. Plant Physiol 82: 280–284

Hardie LP, Balkwill DL and Stevens Jr. SE (1983) Effects of iron starvation on the physiology of the cyanobacterium *Agmenellum quadruplicatum*. Appl Environ Microbiol 45: 999–1006

Hutber GN, Hutson KG and Rogers LJ (1977) Effects of iron deficiency on levels of two ferredoxins and flavodoxin in a cyanobacterium. FEMS Microbiol Lett 1: 193–196

Krupa Z, Williams JP, Khan MU and Huner NPA (1992) The role of acyl lipids in reconstitution of lipid-depleted light-harvesting complex II from cold-hardened and nonhardened rye. Plant Physiol 100: 931–938

Laudenbach DE and Straus NA (1988) Characterization of a cyanobacterial iron stress-induced gene similar to *psbC*. J Bacteriol 170: 5018–5026

Laudenbach DE, Reith ME and Straus NA (1988) Isolation, sequence analysis, and transcriptional studies of the flavodoxin gene from *Anacystis nidulans* R2. J Bacteriol 170: 258–265

Leverenz JW, Falk S, Pilström C-M and Samuelsson G (1990) The effect of photoinhibition on the photosynthetic light response curve of green plant cells (*Chlamydomonas reinhardtii*) Planta 182: 161–168

Ley AC and Mauzerall DC (1982) Absolute absorption cross-sections for Photosystem II and the minimum quantum requirement for photosynthesis in *Chlorella vulgaris*. Biochim Biophys Acta 680: 95–106

Mullineaux C and Allen JF (1986) Fluorescence induction transients indicate dissociation of Photosystem II from the phycobilisome during the state 2 transition in the cyanobacterium *Synechococcus* 6301. Biochim Biophys Acta 934: 96–107

Mullineaux C and Holzwarth AR (1991) Kinetics of energy transfer in the cyanobacterial phycobilisome-Photosystem II complex. Biochim Biophys Acta 1098: 68–78

Öquist G (1971) Changes in pigment composition and photosynthesis induced by iron-deficiency in the blue-green alga *Anacystis nidulans*. Plant Physiol 25: 188–191

Öquist G (1974) Iron deficiency in the blue-green alga *Anacystis nidulans*: Changes in pigmentation and photosynthesis. Physiol Plant 30: 30–37

Pakrasi HB, Goldenberg A and Sherman LA (1985a) Membrane development in the cyanobacterium, *Anacystis nidulans*, during recovery from iron starvation. Plant Physiol 79: 290–295

Pakrasi HB, Riethman HC and Sherman LA (1985b) Organization of pignlent proteins in the Photosystem 11 complex of the cyanobacterium *Anacystis nidulans* R2. Proc Natl Acad Sci USA 82: 6903–6907

Porra RJ, Thompson WA and Kriedemann PE (1989) Determination of accurate extinction coefficients and simultaneous equations for assaying chlorophylls *a* and *b* extracted with four different solvents: verification of the concentration of chlorophyll standards by atomic absorption spectroscopy. Biochim Biophys Acta 975: 384–394

Prentki P and Krisch HM (1984) In vitro insertional mutagenesis with a selecitable DNA fragment. Gene 29: 303–313

Riethman HC, Bullerjahn G, Reddy KJ and Sherman LA (1988) Regulation of cyanobacterial pigment-protein composition and organization by environmental factors. Photosynth Res 18: 133–161

Sambrook J, Fritsch EF and Maniatis T (1989) Molecular Cloning: A Laboratory Manual, Cold Spring Harbor Laboratory Press, Cold Spring Harbor, New York

Sandmann G (1985) Consequences of iron deficiency on photosynthetic electron transport in blue green algae. Photosynth Res 6: 261–271

Troyan TA, Bullerjahn GS, Sherman LA (1989) Assembly of Chl-protein complexes in membranes of iron-stressed *Synechococcus* sp. PCC7942 proceeds in the absence of Chl synthesis. In: Barber J and Malkin R (eds) Techniques and New Developments in Photosynthesis Research, pp 601–604. Plenum Press, New York

Wendler J and Holzwarth AR (1987) State transitions in the green algae *Scenedesmus obliquus* probed by time-resolved chlorophyll fluorescence spectroscopy and global data analysis. Biophys J 52: 717–728

Westall JC, Zachary JL and Morel FMM (1976) MINEQL: A computer program for the calculation of chemical equilibrium composition of aqueous systems. Technical note no. 18, RM Parsons Lab for Water Res and Env Eng, Massachusetts Institute of Technology, Cambridge, 91 pp

Williams JGK (1988) Construction of specific mutations in Photosystem II photosynthetic reaction center by genetic engineering methods in lit Synechocystis 6803. Methods Enzymol 167: 766–778

Zhao J and Brand JJ (1989) Specific bleaching of phycobiliproteins from cyanobacteria and red algae at high temperature in vivo. Arch Microbiol 152: 447–452